Atmos. Meas. Tech. Discuss., https://doi.org/10.5194/amt-2019-39
Manuscript under review for journal Atmos. Meas. Tech.
Discussion started: 6 March 2019

Atmospheric Measurement Techniques Discussions

Inter-comparison between the Aerosol Optical Properties Retrieved by Different Inversion Methods from SKYNET Sky Radiometer Observations over Qionghai and Yucheng in China

Zhe Jiang[1], Minzheng Duan[1*], Huizheng Che[2*], Wenxing Zhang[1], Teruyuki Nakajima[3], Makiko Hashimoto[3], Bin Chen[1], and Akihiro Yamazaki[4]

[1]Institute of Atmospheric Physics, Chinese Academy of Sciences, Beijing 100029, China
[2]State Key Laboratory of Severe Weather (LASW) and Institute of Atmospheric Composition, Chinese Academy of Meteorological Sciences (CAMS), CMA, Beijing 100081, China
[3]Earth Observation Research Center (EORC), Japan Aerospace Exploration Agency (JAXA), Tsukuba, Ibaraki 305-8505, Japan
[4]Japan Meteorological Agency, Meteorological Research Institute, 1-1 Nagamine, Tsukuba, Ibaraki 305-0052, Japan

Correspondence to: Huizheng Che(chehz@cma.gov.cn) and Minzheng Duan(dmz@mail.iap.ac.cn)

Abstract. This study analyzed the aerosol optical properties derived by SKYRAD.pack versions 5.0 and 4.2 using the radiometer measurements over Qionghai and Yucheng in China, two new sites of the sky radiometer network (SKYNET). The volume size distribution retrieved by V5.0 presented bimodal patterns with a 0.1–0.2 μm fine particle mode and a 5–6 μm coarse particle mode both over Qionghai and Yucheng. The differences of the volume size distributions between the two versions were very large for the coarse mode with a radius of over 5 μm. The mean values of single scattering albedo (SSA) at 500 nm retrieved from V5.0 were approximately 0.02 lower, but 0.03 higher than those from V4.2 in Qionghai and Yucheng, respectively. The average imaginary part of the complex refractive index (m_i) retrieved from V5.0 at all wavelengths was systemically higher than those by V4.2 over Qionghai. Moreover, the differences between the real parts of the complex refractive index (m_r) obtained using the two versions were within 4.25% both at Yucheng and Qionghai. The seasonal variability of the aerosol properties over Qionghai and Yucheng were investigated based on SKYRAD.pack V5.0. The seasonal average SSA during the winter was larger than those in other seasons in Yucheng, while the lowest SSA values occurred in winter over Qionghai. Meanwhile, the m_r showed a minimum in winter over both sites. The results can provide validation data in China for SKYNET to continue improving the data-processing and inversion method. The results provide valuable references for continued improvement of the retrieval algorithms of SKYNET and other aerosol observational networks.

Atmos. Meas. Tech. Discuss., https://doi.org/10.5194/amt-2019-39
Manuscript under review for journal Atmos. Meas. Tech.
Discussion started: 6 March 2019

Atmospheric Measurement Techniques Discussions

1 Introduction

Aerosols are well known to have significant impacts on climate change and global hydrologic cycle by absorbing, scattering, and reflecting solar radiation (Hansen et al., 1997; Sun et al., 2017) and participating in cloud processes (Ackerman et al., 2000; Ramanathan et al., 2001; Kaufman et al., 2005; Li et al., 2011; Bi et al., 2014; Zhao et al., 2018a). Aerosols also adversely influence human health and visibility (Samet et al., 2000; Pope lii et al., 2002; Yang et al., 2015; Wang et al., 2017), aerosol-related problems have drawn a great deal of attention (Cai et al., 2016).

Using a sun/sky radiometer to measure both direct solar beam and angular sky radiance is the most common method for a reliable and continuous estimate of detailed aerosol properties over mega-cities around the world. Many aerosol ground-based observation networks were established to understand the aerosol optical properties, validate the inversion products of satellite remote sensing, and indirectly evaluate their effect on climate (Uchiyama et al., 2005; Takamura and Nakajima, 2004; Nakajima et al., 2007). SKYNET, the focus of this study, is a ground-based research network of using sky radiometers (PREDE Co., Ltd., Tokyo, Japan) with observation sites principally located in Asia and Europe (Che et al., 2014).

The direct solar and angular sky radiance data measured by the sky radiometers are processed to obtain the aerosol optical properties, such as aerosol optical depth (AOD), single scattering albedo (SSA), complex refractive index, and volume size distribution function (SDF) using SKYRAD.pack, which is the official retrieval algorithm of the SKYNET network (Nakajima et al., 1996) having several different versions. SKYNET currently uses the SKYRAD.pack algorithm version 4.2 (Takamura and Nakajima, 2004). The aerosol retrievals derived from SKYRAD.pack version 4.2 algorithm have been used to investigate the regional and seasonal characteristics of aerosols for climate and environmental studies and validate satellite remote sensing results (e.g., Kim et al., 2004; Che et al., 2008; Campanelli et al., 2010; Estellés et al., 2012a; Wang et al., 2014; Che et al., 2018). Recently, a new SKYRAD.pack version 5.0 was proposed to improve SSA retrievals (Hashimoto et al., 2012), there are few applications of SKYRAD V5.0 in China, and it was just preliminarily used to retrieve aerosol optical properties over Beijing in China (Che et al., 2014).

This study presents the aerosol optical properties over Qionghai and Yucheng by using SKYRAD.pack V5.0 and V4.2 from SKYNET sky radiometer measurements during February 2013 to February 2015.

This work is designed to achieve the following objectives: (1) investigate the difference of the aerosol optical properties derived by SKYRAD.pack V5.0 and V4.2 over the two SKYNET sites; and (2) analyze the seasonal variability of aerosol optical properties over Qionghai and Yucheng based on SKYRAD.pack V5.0. The results presented in this study provide valuable references for continued improvement of the retrieval algorithms of SKYNET and other aerosol observational networks.

2 Site description, instrumentation, and inversion method

2.1 Site Geo-information and Instrumentation

The sky radiometer (Model POM-02, PREDE Co. Ltd.) was deployed at Qionghai and Yucheng from February 2013 and January 2013, respectively. The PREDE-POM02 model was equipped with an InGaAs detector to measure the direct solar irradiance and the sky diffuse radiance at 11 wavelengths, namely, 315, 340, 380, 400, 500, 675, 870, 940, 1020, 1627, and 2200 nm. The data from five channels at 400, 500, 675, 870, and 1020 nm were used here to retrieve the aerosol optical properties over Qionghai and Yucheng. The full angle field of view is 1.0°, while the minimum scattering angle of measurement is approximately 3°. The sky radiance is measured at 24 predefined scattering angles and at regular time intervals. The sky radiometer operates only during daytime and collects data regardless of the sky conditions. Its dynamic range is 107. The typical measurement interval is 10 min. The precision of the in-situ method was estimated to be within 1–2.5% depending on the wavelength (Campanelli et al., 2004).

The Qionghai site of SKYNET (19.23°N, 110.46°E, 24 m a.s.l.), which was located in the eastern part of Hainan Island, had a humid climate and an abundant precipitation. The observations at this site could represent the aerosol characteristics of the land and sea border area in south China. The observation at the Yucheng site (36.82°N, 116.57°E, 22 m a.s.l.) could represent the aerosol properties of farmland areas in North China Plain.

2.2 Inversion method

The aerosol optical properties (i.e., AOD, SSA, complex refractive index, and volume SDF) were derived in this study by using SKYRAD.pack V4.2 and V5.0. Within the SKYRAD.pack code, the inversion schemes were used to derive the single scattering term $\beta(\Theta)$ from the measurements of the normalized sky flux $R(\Theta)$ and retrieve the aerosol SDF $v(r)$ (as a function of particle radius, r) from data $\beta(\Theta)$ and AOD τ. The inversion of $\beta(\Theta)$ was performed through a non-linear iterative method. Each step

Atmos. Meas. Tech. Discuss., https://doi.org/10.5194/amt-2019-39
Manuscript under review for journal Atmos. Meas. Tech.
Discussion started: 6 March 2019

of the loop contained the procedure for retrieving v(r) using a constrained linear or a non-linear iterative method.

The retrieved v(r) in each iteration step was used as an input parameter for the radiative transfer model (Nakajima and Tanaka, 1988) to simulate R(Θ), which was compared with the measured R(Θ) to evaluate the root mean square difference ε(R). The maximum number of iterations and the tolerance parameter for the convergence of R were set as 20 and 0.1%, respectively.

The retrieval of v(r) from β(Θ) and τ data in SKYRAD.pack V4.2 was conducted using a constrained linear method. The inversion method consisted of a linear matrix formulation, in which the solution stability was controlled by the requirement that it agrees both with the input data and the imposed weighted constraints (Nakajima et al., 1983).

$$f=Kx+\varepsilon. \quad (1)$$

where f is the vector of the β(Θ) and τ data, and x is a state vector containing the values of size distribution vi = v(r_i) with r_i equidistant on a logarithmic scale (i.e., ln (r_{i+1}) − ln (r_i) = const. The components of vector ε were the error of each datum, K = K (m(λ)), a matrix of the kernel coefficients calculated for the fixed values of the complex refractive index (m(λ)).

V4.2 used the iterative relaxation method of Nakajima et al. (1983, 1996) to remove the multiple scattering contribution and derived an optimal solution using a statistical regularization method (Turchin and Nozik, 1969) by minimizing the following cost function as proposed by Phillips (1962) and Twomey (1963):

$$e^2=|(f-Kx)|^2+\gamma|Bx|^2. \quad (2)$$

where B is a smoothing matrix used to generate a priori information that forces the solution x to be a smooth function of ln(r); and γ is a Lagrange multiplier coefficient to minimize the first term of the right-hand side of Eq. (2). The solution of Eq. (1) provided a smooth retrieval of the size distribution v(r) corresponding to the minimum of e2 defined by Eq. (2). In such an approach, both the solution v(r) and e2 depended on the assumed value of the complex refractive index m(λ). The complex refractive index m(λ) in each iteration was also evaluated together with v(r), but the retrieved m(λ) can only be chosen from the predefined set of values.

The m(λ) values in SKYRAD.pack V5.0 were directly included in the state vector x. Eq. (1) becomes non-linear, and V5.0 solved it using the non-linear maximum likelihood method defined by Rodgers (2000). This method was based on the Bayesian theory.

$$p(x|f)=p(f|x)p(x)/p(f) . \quad (3)$$

where p is the probability density function defined as the Gaussian distribution; and x and f denote the state and measurement vectors, respectively. Accordingly, x was chosen in the maximum likelihood method, such that the posterior probability p(x|f) becomes the maximum under the condition that a priori information is already given. We obtained the following equation in the tangential space to be solved by a Newtonian method by organizing this non-linear equation, such that p(x|f) = max:

$$x_{k+1}=x_k+(U_k^T S_e^{-1} U_k+S_a^{-1})^{-1}[U_k^T S_e^{-1}(f-f_k)- S_a^{-1}(x_k-x_a)] . \quad (4)$$

where x_k is the solution at the k^{th} iteration step; $f_k=f(x_k)$ is an observation modeled using x_k ; x_a is the a priori value of x; S_e is the measurement error covariance matrix; S_a denotes the covariance matrix

Atmos. Meas. Tech. Discuss., https://doi.org/10.5194/amt-2019-39
Manuscript under review for journal Atmos. Meas. Tech.
Discussion started: 6 March 2019

Atmospheric Measurement Techniques Discussions

defined by a priori and state values, $S_a=(x-x_a)(x-x_a)^T$; and U is the Jacobi matrix, $\partial f/\partial x$. The retrieval algorithm used in V5.0 allowed a rigorous retrieval of both the aerosol size distribution and the spectral complex refractive index.

The non-linear inversion has a strong dependence on the estimation of the first-guess solution. Version 5.0 uses an a priori SDF of a bimodal log-normal function as follows:

$$v(r) = \sum_{n=1}^{2} C_n \exp\left[-\frac{1}{2}\left(\frac{\ln r - \ln r_{mn}}{\ln S_n}\right)^2\right] . \quad (5)$$

where r_{m1} = 0.1 μm; r_{m2}= 2.0 μm; S_1 = 0.4; S_2 = 0.8; $C_1 = 1.0 * 10^{-12}$; and $C_2 = 1.0 * 10^{-12}$, following the reported climate values (Higurashi et al., 2000). For the a priori estimates of the refractive index, the real (m_r) and imaginary (m_i) parts were set as m_r = 1.5 and m_i = 0.005, respectively. SKYRAD V5.0 developed a stricter data quality control method of observation data and cloud screening.

3 Results and discussion

The results retrieved by SKYRAD.pack V4.2 were used to compare with the results retrieved by SKYRAD.pack V5.0. The inter-comparisons of the volume size distribution, single scatter albedo, and refractive index between V5.0 and V4.2 were based on 2517 measurements for 349 days over Qionghai and 6502 measurements for 307 days over Yucheng. Considering a relatively low retrieval accuracy of SSA when AOD < 0.2 (Hashimoto et al., 2012), only the measurements with AOD > 0.2 were selected to be effective values in this study.

3.1 Inter-comparison of the volume size distribution results between SKYRAD V4.2 and V5.0

Aerosol size properties are one of the most important sources of information for both the observation and modeling of radiative forcing (Dusek et al., 2006). The volumes at each bin were monthly averaged during the experiment period, for V4.2 and V5.0 over Qionghai and Yucheng (Figs. 1a, b). As V5.0 uses an a priori SDF of a bimodal log-normal function (Hashimoto et al., 2012), the volume SDF derived by V5.0 generally showed the classic bi-mode patterns at both Qionghai and Yucheng. The SDF from V5.0 showed two peaks at radii of 0.17 μm and 5.29 μm at the two sites. The SDF retrieved by V4.2, was generally similar to V5.0 at radius < 5 μm. However, V4.2 showed a predominant peak at the coarse mode with a radius over 10 μm. The large differences at radius over 5 μm are probably because of the strong constraint on the SDF for the coarse mode particles applied in V5.0 (Hashimoto et al., 2012). Figures 1a and b showed that there were larger differences in volume SDF of the coarse mode between V4.2 and V5.0 at Qionghai than those at Yucheng.

Atmos. Meas. Tech. Discuss., https://doi.org/10.5194/amt-2019-39
Manuscript under review for journal Atmos. Meas. Tech.
Discussion started: 6 March 2019

Atmospheric Measurement Techniques Discussions

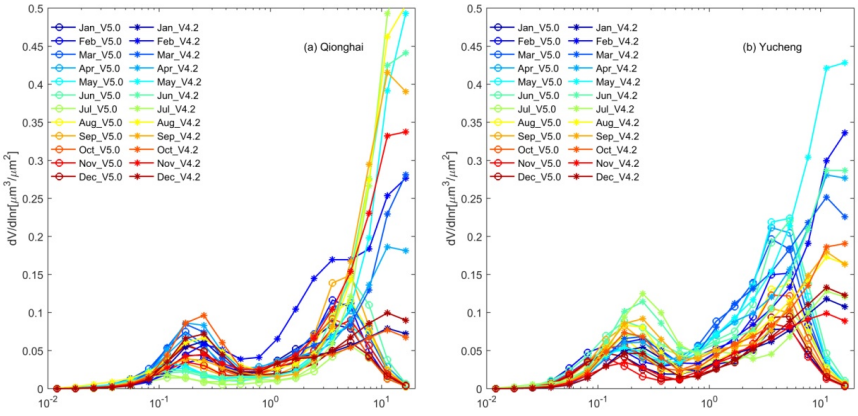

Figure 1: Retrieved monthly volume size distribution between SKYRAD V4.2 and V5.0 for Qionghai (a) and Yucheng (b) during February 2013 to February 2015.

3.2 Inter-comparison of the single scatter albedo results between SKYRAD V4.2 and V5.0

As a key variable in assessing the climatic effects of aerosols, the SSA is defined as the ratio of the scattering coefficient and the extinction coefficient. It characterized the absorption properties of aerosols and an important quantity in evaluating aerosol radiative forcing. The SSA value is mostly dependent on the shape, size distribution, and concentration of the aerosol particles.

Tables 1 and 2 present average single scattering albedo and refractive index for SKYRAD 5.0 and 4.2 and the differences between the two versions over Qionghai and Yucheng during February 2013 to February 2015, respectively. The percentage differences of SSA between SKYRAD V4.2 and V5.0 at 400, 500, 675, 870, and 1020 nm over Qionghai were −3.28%, −2.05%, −0.36%, −2.07%, and −1.79%, respectively. Over the Yucheng station, the SSA retrieved from V5.0 were approximately 0.02 (2.48%), 0.03(3.74%), and 0.06 (6.60%) lower at 400, 870, and 1020 nm, but 0.03 (3.19%) and 0.02 (2.22%) larger at 500 and 675 nm, respectively, than those from V4.2.

Figures 2a and b present the monthly mean SSA at 500 nm over Qionghai and Yucheng, respectively. The SSA values computed from V5.0 were lower than those from V4.2 over Qionghai in all months except July. However, the monthly averaged SSA results by V5.0 were higher than those from V4.2 except for September at the Yucheng site.

Atmos. Meas. Tech. Discuss., https://doi.org/10.5194/amt-2019-39
Manuscript under review for journal Atmos. Meas. Tech.
Discussion started: 6 March 2019

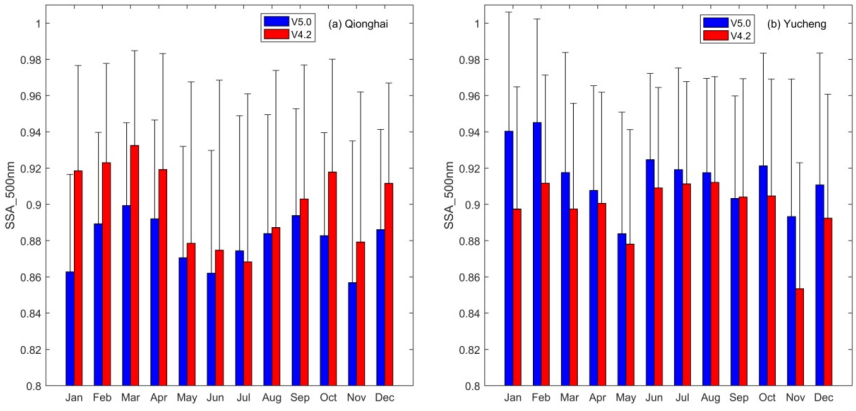

Figure 2: Comparison of the monthly mean values of the single scattering albedo (SSA) at 500 nm between SKYRAD V4.2 and V5.0 for Qionghai (a) and Yucheng (b) during February 2013 to February 2015.

3.3 Inter-comparison of the refractive index results between SKYRAD V4.2 and V5.0

The real part of the refractive index (m_r) represents scattering. A higher m_r indicates a higher scattering. The imaginary part of the refractive index (m_i) represents absorption of the aerosols and is an important quantity in evaluating the aerosol radiative forcing.

Contrary to the single scattering albedo, the averaged m_i retrieved from V5.0 at all wavelengths were systemically higher than those by V4.2 over Qionghai (Table 1). The mean values of m_i retrieved from V4.2 were approximately 0.007, 0.005, 0.002, 0.005, and 0.005 lower than those from V5.0 for the five channels of 400, 500, 675, 870, and 1020 nm, respectively, over Qionghai. The averaged m_i retrieved by V5.0 was 0.003, 0.005, and 0.008 higher at 400, 870, and 1020 nm wavelengths, respectively, but 0.005 and 0.003 lower at 500 and 675 nm, respectively, than those retrieved by V4.2 in Yucheng.

The frequency distributions of m_i values at 500nm retrieved by V5.0 and V4.2 are given in Fig. 3a and b for all the instantaneous data. In Qionghai site, the frequency histogram of m_i by V4.2 shows a unimodal distribution with a maximum frequency of about 40% in the range of 0 to 0.005. The probability distribution of m_i by V5.0 is different; it is relatively uniform within the whole range from 0 to 0.03. As shown in Fig. 3b, the frequency distributions of V5.0 and V4.2 over Yucheng site indicate a similar decreasing trend with increasing m_i. The accumulated frequency in the range from 0 to 0.01 is about 60% for V4.2 and 78% for V5.0.

Generally, the difference in m_r between the two versions was smaller than that in m_i (Tables 1 and 2). The results for the real part of the complex refractive index (m_r) showed that m_r at wavelengths of 400,

Atmos. Meas. Tech. Discuss., https://doi.org/10.5194/amt-2019-39
Manuscript under review for journal Atmos. Meas. Tech.
Discussion started: 6 March 2019

Atmospheric Measurement Techniques Discussions

500, and 675 nm by V5.0 were lower than those by V4.2, but larger than those by V4.2 at 870 and 1020 nm over Yucheng. The mean values of m_r retrieved by V5.0 were approximately 0.023 (1.52%), 0.042 (2.78%), and 0.023 (1.51%) lower than V4.2 at 400, 500, and 675 nm, but 0.006 (3.70%) and 0.026 (1.70%) larger than V4.2 at 870 and 1020 nm, at the Yucheng station. The m_r values by V5.0 were mostly larger than those by V4.2 at the five wavelengths over Qionghai. The mean m_r from V5.0 were approximately 0.06 (4.24%), 0.034 (2.35%), 0.018 (1.27%), 0.021 (1.42%), and 0.016 (1.08%) higher than those from V4.2 over the Qionghai station. The percentage differences of the mean m_r obtained using the two versions were all within 4.25% both at Yucheng and Qionghai.

Figures 4a and b show the frequency distribution of the m_r values at 500nm derived from V5.0 and V4.2 over Qionghai and Yucheng, respectively. The values of m_r retrieved by V5.0 over the two sites both show unimodal distributions with peaks occurring within the range from 1.45 to 1.5. For the m_r values by V4.2, the accumulated occurrences in the range from 1.35 to 1.5 are about 90% over Qionghai. Approximately 65 % of m_r values by V4.2 are between 1.45 and 1.55 over Yucheng.

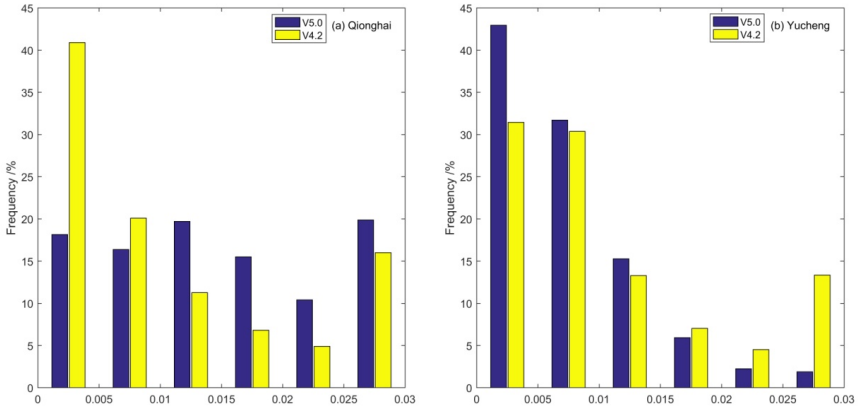

Figure 3: The frequency distributions of the imaginary part of the complex refractive index (m_i) at 500nm for SKYRAD V4.2 and V5.0 over Qionghai (a) and Yucheng (b).

Atmos. Meas. Tech. Discuss., https://doi.org/10.5194/amt-2019-39
Manuscript under review for journal Atmos. Meas. Tech.
Discussion started: 6 March 2019

Atmospheric Measurement Techniques Discussions

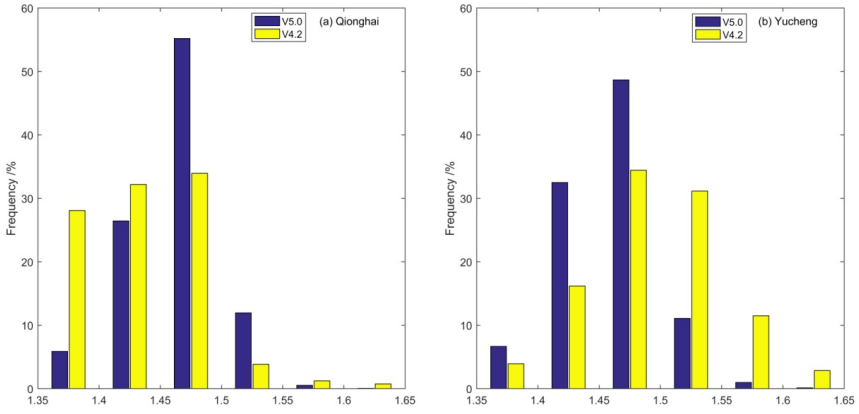

Figure 4: The frequency distributions of the real part of the complex refractive index (m_r) at 500nm for SKYRAD V4.2 and V5.0 over Qionghai (a) and Yucheng (b).

3.4 Seasonal variability of the aerosol optical properties over Qionghai and Yucheng based on SKYRAD.pack V5.0

The analysis of the 500 nm channel was chosen because it was widely quoted in sun photometric and remote sensing applications and generally representative of visible band wavelengths (Estellés et al., 2012b). Four seasons were considered in this paper (i.e., spring (March–May), summer (June–August), autumn (September–November), and winter (December–February)) to investigate the seasonal variations of the aerosol optical properties over Qionghai and Yucheng based on SKYRAD.pack V5.0.

3.4.1 AOD

The AOD was representative of the aerosol loading in the atmospheric column and important for the identification of the aerosol source regions and the aerosol evolution.

The AOD showed a distinct seasonal variation over both Qionghai and Yucheng. Figure 5a showed that the seasonal averaged AOD over Qionghai had higher values in spring, winter and autumn while lower in summer. The background wind in Qionghai is the northeasterly wind from November through April, and the wind would import pollutants from South China into Hainan. In Yucheng, the AOD averages were commonly higher in summer and spring than in winter and autumn, the maximum average of 0.98 occurring in summer maybe was caused by hygroscopic effects. The high AOD in spring was likely related to the long-range transportation of dust from northern/northwestern China.

Atmos. Meas. Tech. Discuss., https://doi.org/10.5194/amt-2019-39
Manuscript under review for journal Atmos. Meas. Tech.
Discussion started: 6 March 2019

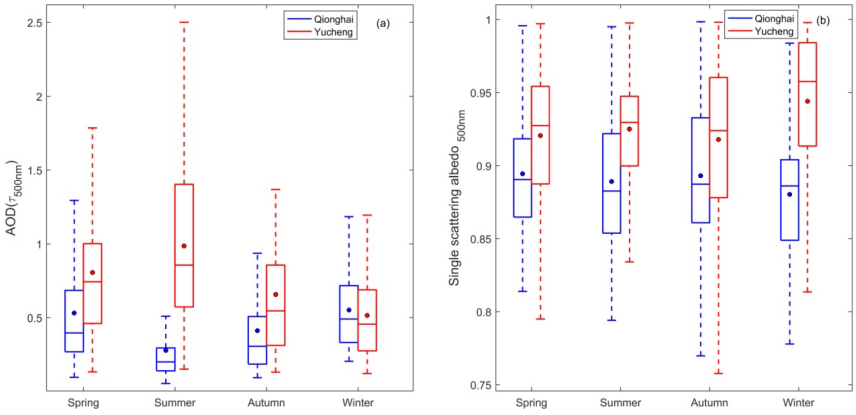

Figure 5: Seasonal variations in the AOD (a) and the single scattering albedo (SSA) (b) based on SKYRAD V5.0 over Qionghai and Yucheng for the period from February 2013 to February 2015. The boxes represent the 25th to 75th percentiles of the distributions while the dots and solid lines within each box represent the means and medians, respectively.

3.4.2 SSA

Figure 5b shows the seasonal averaged SSA at 500 nm for Qionghai and Yucheng during 2013–2015. The SSA values showed a relatively uniform seasonal distribution in Qionghai. The SSA averages were approximately 0.90, 0.89, 0.89, and 0.88 in spring, summer, autumn, and winter, respectively. The mean SSA at 500 nm in Yucheng was significantly larger than that in Qionghai. The highest and lowest monthly average SSAs in Yucheng were found in February (0.97) and November (0.89) respectively. The seasonal mean SSA during the winter was larger than those in other seasons. Unlike the highest SSA value found in winter, the lowest SSA over Qionghai appeared in winter, it was mainly caused by the increase of the absorbing aerosol.

3.4.3 Volume Size Distribution

Figures 6a and b show the seasonal averaged volumes of the different aerosol particle size distributions ($dv/d\ln r$) in Qionghai and Yucheng. The aerosol volume size distributions were typical bimodal patterns during each season at the Qionghai and Yucheng sites. Figures 6 show that there was a larger contribution of coarse-mode particles to the aerosol volume compared with the fine-mode particles at the two sites. The fine mode showed a peak at a radius of 0.17 μm in all seasons over Qionghai. The coarse mode was characterized by a peak at a radius of 5.29 μm in spring, summer, and autumn and 3.62 μm in winter. The size distributions showed distinct differences in their dominant modes for the

Atmos. Meas. Tech. Discuss., https://doi.org/10.5194/amt-2019-39
Manuscript under review for journal Atmos. Meas. Tech.
Discussion started: 6 March 2019

Atmospheric Measurement Techniques Discussions

different seasons. As shown in Fig. 6a, the fraction of the fine aerosol particles was much smaller in summer than for the other seasons. Meanwhile, the fraction of the coarse mode aerosol particles was larger than that in spring and winter probably because of the monsoonal influence, increase of the sea salt particles of a relatively large size, and decrease of the anthropogenic aerosol.

As shown in Fig. 6b, the coarse-mode particle in Yucheng has a much larger spread compared to the volume distribution of the fine-mode particle. In spring, the volume of the coarse aerosol particles relative to the whole was much larger than for the other seasons in Yucheng probably because of the presence of the dust particles transported from the northwest of China (Zhao et al., 2018b).

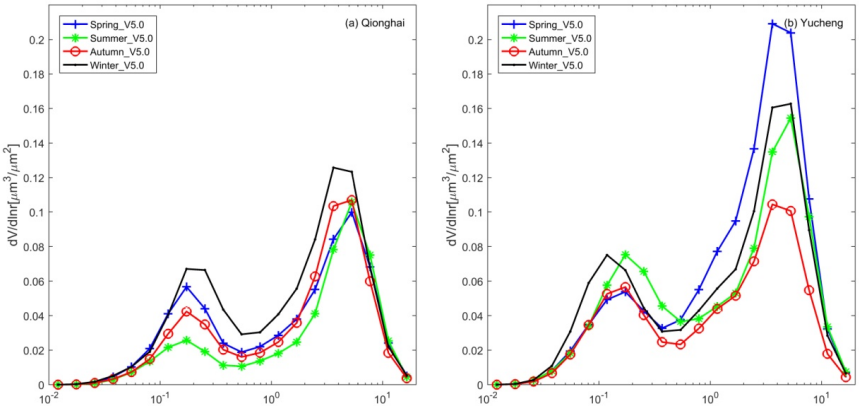

Figure 6: Seasonally averaged volumes of the different aerosol particle size distributions based on SKYRAD V5.0 over Qionghai (a) and Yucheng (b) for the period from February 2013 to February 2015.

3.4.4 Refractive index

Figure 7a shows the seasonal variation of the real part of the refractive index at 500 nm over Qionghai and Yucheng. The averages of the real parts were higher in spring compared to the other seasons, especially in Yucheng. The m_r in Yucheng showed a maximum of approximately 1.4719 in spring and a minimum of approximately 1.4476 in winter. The averages of the real part at 500 nm in Qionghai were 1.4686, 1.4675, 1.4514, and 1.4464 in spring, summer, fall, and winter, respectively.

Figure 7b presents the seasonal variation of the imaginary part of the refractive index at 500 nm over Qionghai and Yucheng. The imaginary part of the refractive index in Yucheng was higher in summer and autumn than those of spring and winter. The highest value was 0.0089 in summer, and the low values were 0.0059 and 0.0042 in spring and winter, respectively. Contrary to the seasonal variation trend of m_i at Yucheng, the m_i values in Qionghai were lower in summer and autumn than those in

Atmos. Meas. Tech. Discuss., https://doi.org/10.5194/amt-2019-39
Manuscript under review for journal Atmos. Meas. Tech.
Discussion started: 6 March 2019

Atmospheric Measurement Techniques Discussions

spring and winter.

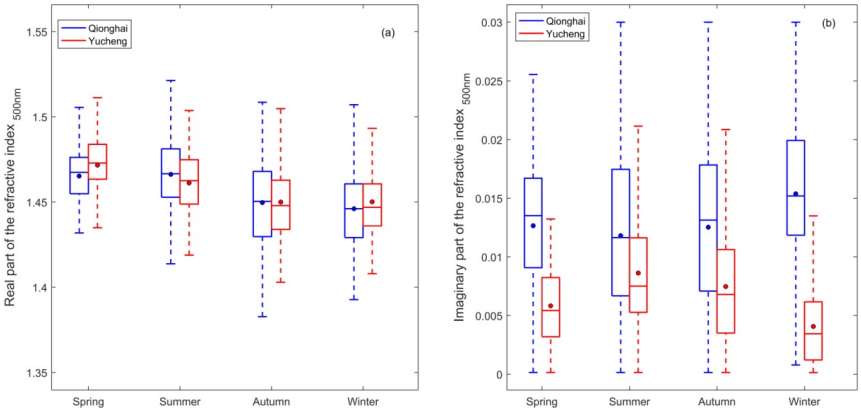

Figure 7: Seasonal variations in the real part of the refractive index (a) and the imaginary part of the refractive index (b) based on SKYRAD V5.0 over Qionghai and Yucheng for the period from February 2013 to February 2015. The boxes represent the 25th to 75th percentiles of the distributions while the dots and solid lines within each box represent the means and medians, respectively.

4 Summary

The aerosol optical properties over the two new SKYNET sites of Qionghai and Yucheng in China were continuously investigated over two years using the RREDE-POM02 sky radiometer measurements. The volume size distribution retrieved by V5.0 presented an overall bimodal pattern with a 0.10–0.20 μm fine particle mode and a 5.0–6.0 μm coarse particle mode both over Qionghai and Yucheng. The SSA retrieved by V5.0 at 400, 500, 675, 870, and 1020 nm over Qionghai was −3.28%, −2.05%, −0.36%, −2.07%, and −1.79% lower than the retrievals of V4.2. The mean values of SSA retrieved from V5.0 were approximately 0.02 (2.48%), 0.03 (3.74%), and 0.06 (6.60%) lower at 400, 870, and 1020 nm, respectively, but 0.03 (3.19%) and 0.02 (2.22%) larger at 500 and 675 nm, respectively, than those from V4.2 over the Yucheng station. The real and imaginary parts of the refractive index between V5.0 and V4.2 compared very different in the two sites, probably due to the different compositions of aerosol over Qionghai and Yucheng.

Based on SKYRAD.pack V5.0, the seasonal variations of the aerosol optical properties over Qionghai and Yucheng were investigated. The seasonal patterns of AOD were quite different between the two stations. The AOD showed high values in winter and spring but decreased to minimum in summer over Qionghai. But in Yucheng, the maximum AOD at 500 nm of approximately 0.98

appeared in summer. The seasonal SSA values showed a rather uniform seasonal distribution in Qionghai. The SSA averages were approximately 0.90, 0.89, 0.89, and 0.88 in spring, summer, autumn, and winter, respectively. The seasonal average SSA during the winter was larger than those in other seasons over Yucheng. The fine modes showed a peak at a radius of about 0.17 μm in all seasons over Qionghai, while the coarse modes showed peaks at a radius of 5.29 μm in spring, summer, and autumn and 3.62 μm in winter. In Yucheng, the volume of the coarse aerosol particles relative to the whole was much larger than for the other seasons in spring, probably due to the presence of the dust particles transported from the northwest of China.

The comparison results between the aerosol optical properties retrieved by SKYRAD5.0 and SKYRAD4.2 were very different over the two SKYNET sites. The results can provide validation data in China for SKYNET to continue improving data-processing and inversion method. Meanwhile, the results can promote the integration of more Chinese observation stations into international network.

Data availability. The sky radiometer data at Qionghai and Yucheng, China are available on request by contacting the first author of the paper (jiangzhe@mail.iap.ac.cn).

Author contributions. Zhe Jiang and Huizheng Che designed the present study, Minzheng Duan and Wenxing Zhang performed observation, Zhe Jiang analyzed data and wrote the paper, with support from all the authors. Teruyuki Nakajima designed the inversion method and Makiko Hashimoto improved the inversion method. Teruyuki Nakajima, Makiko Hashimoto, Bin Chen and Akihiro Yamazaki gave useful comments.

Competing interests. The authors declare that they have no conflict of interest.

Acknowledgements. This work was supported by the National Key Research and Development Program of China (2017YFB0503603) and the National Natural Science Foundation of China (41825011, 41301381, 41475026 and 41705014).

References

Ackerman, A. S., Toon, O. B., Stevens, D. E., Heymsfield, A.J., Ramanathan, V., and Welton E.J.: Reduction of tropical cloudiness by soot, Science, 288, 1042–1047, doi: 10.1126/science.288.5468.1042, 2000.

Bi, J. R., Shi, J. S. , Xie, Y. K., and Liu Y. Z.: Dust Aerosol Characteristics and Shortwave

Radiative Impact at a Gobi Desert of Northwest China during the Spring of 2012, J. Meteor. Soc. Japan, 92A, 33–56, doi: 10.2151/jmsj.2014-A03, 2014.

Cai J. X., Guan, Z. Y. , and Ma, F. H. : Possible combined influences of absorbing aerosols and anomalous atmospheric circulation on summertime diurnal temperature range variation over the middle and lower reaches of the Yangtze River, J. Meteor. Res., 30(6), 927–943,doi: 10.1007/s13351-016-6006-1, 2016.

Campanelli, M., Nakajima, T., and Olivieri, B.: Determination of the solar calibration constant for a sun-sky radiometer: Proposal of an in-situ procedure, Appl. Opt., 43, 651–659, doi:10.1364/AO.43.000651, 2004.

Campanelli, M., Lupi, A., Nakajima, T., Malvestuto, V., Tomasi, C., and Estelles, V.: Summertime columnar content of atmospheric water vapor from ground-based Sun-sky radiometer measurements through a new in situ procedure, J. Geophys. Res., 115, D19304, doi:10.1029/2009JD013211, 2010.

Che, H., Shi, G., Uchiyama, A., Yamazaki, A., Chen, H., Goloub, P., and Zhang, X.: Intercomparison between aerosol optical properties by a PREDE skyradiometer and CIMEL sunphotometer over Beijing, China, Atmos. Chem. Phys., 8, 3199–3214, doi:10.5194/acp-8-3199-2008, 2008.

Che, H. Z., Xia, X. A., Zhu, J., Wang, H., Wang, Y. Q., Sun, J.Y., Zhang, X. C., Zhang, X. Y., and Shi, G. Y.: Aerosol optical properties under the condition of heavy haze over anurban site of Beijing, China, Environ. Sci. Pollut. R., 22, 1043–1053, https://doi.org/10.1007/s11356-014-3415-5, 2014.

Che, H. Z., Qi, B., Zhao, H. J., Xia, X. A., Eck, T. F., Goloub, P., Dubovik, O., Estelles, V., Cuevas-Agulló, E., Blarel, L., Wu, Y. F., Zhu, J., Du, R. G., Wang, Y. Q., Wang, H., Gui, K., Yu, J., Zheng, Y., Sun, T. Z., Chen, Q. L., Shi, G. Y., and Zhang, X. Y..: Aerosol optical properties and direct radiative forcing based on measurements from the China Aerosol Remote Sensing Network (CARSNET) in eastern China, Atmos. Chem. Phys., 18, 405–425, doi:10.5194/acp-18-405-2018, 2018.

Dusek, U., Frank, G. P., Hildebrandt, L., Curtius, J., Schneider, J., Walter, S., Chand, D., Drewnick, F., Hings, S., Jung, D., Borrmann, S., and Andreae, M. O.: Size matters more than chemistry for cloud-nucleating ability of aerosol particles, Science, 312(5778), 1375–1378, doi:10.1126/science.1125261, 2006.

Estellés, V., Campanelli, M., Utrillas, M. P., Expósito, F., and Martínez-Lozano, J. A.: Comparison of

AERONET and SKYRAD4.2 inversion products retrieved from a Cimel CE318 sunphotometer, Atmos. Meas. Tech., 5, 569–579, https://doi.org/10.5194/amt-5-569-2012, 2012a.

Estellés, V., Smyth, T. J., Campanelli, M.: Columnar aerosol properties in a Northeastern Atlantic site (Plymouth,United Kingdom) by means of ground based skyradiometer data during years 2000-2008, Atmos. Environ., 61, 180–188, doi :10.1016/j.atmosenv.2012.07.024, 2012b.

Hashimoto, M., Nakajima, T., Dubovik, O., Campanelli, M., Che, H., Khatri, P., Takamura, T., and Pandithurai, G.: Development of a new data-processing method for SKYNET sky radiometer observations, Atmos. Meas. Tech., 5, 2723–2737, https://doi.org/10.5194/amt-5-2723-2012, 2012.

Hensen, J., Sato, M., and Ruedy, R.: Radiative forcing and climate response, J. Geophys. Res., **102**(D6), 6831–6864, doi:10.1029/96JD03436, 1997.

Higurashi, A., Nakajima, T., Holben, B., Smirnov, A., Frouin, R., and Chatenet, B.: A study of global aerosol optical climatology with two channel AVHRR remote sensing, J. Climate, 13, 2011–2027, 2000.

Kaufman, Y. J., Koren, I., Remer, L. A., Rosenfeld, D., and Rudich, Y.: The effect of smoke, dust, and pollution aerosol on shallow cloud development over the Atlantic Ocean, Proc. Natl. Acad. Sci. U.S.A., 102, 11207–11212, doi: 10.1073/pnas.0505191102, 2005.

Kim, D. H., Sohn, B. J., Nakajima, T., Takamura, T., Takemura, T., Choi, B. C., and Yoon, S. C.: Aerosol optical properties over east Asia determined from ground-based sky radiation measurements, J. Geophys. Res., 109, D02209, doi:10.1029/2003JD003387, 2004.

Nakajima, T., Tanaka, M., and Yamauchi, T.: Retrieval of the optical properties of aerosols from the aureole and extinction data, Appl. Optics, 22, 2951–2959, doi: 10.1364/AO.22.002951, 1983.

Nakajima, T. and Tanaka, M.: Algorithms for radiative intensity calculations in moderately thick atmospheres using a truncation approximation, J. Quant. Spectrosc. Ra., 40, 51–69, doi: 10.1016/0022-4073(88)90031-3, 1988.

Nakajima, T., Tonna, G., Rao, R., Kaufman, Y., and Holben, B.: Use of sky brightness measurements from ground for remote sensing of particulate polydispersions. Appl. Optics, 35, 2672–2686, doi: 10.1364/AO.35.002672, 1996.

Nakajima, T., Yoon, S. C., Ramanathan, V., Shi, G. Y., Takemura, T., Higurashi, A., Takamura, T., Aoki, K., Sohn, B. J., Kim, S. W., Tsuruta, H., Sugimoto, N., Shimizu, A., Tanimoto, H., Sawa, Y., Lin, N. H., Lee, C. T., Goto, D., and Schutgens, N.: Overview of the Atmospheric Brown Cloud East

Asian Regional Experiment 2005 and a study of the aerosol direct radiative forcing in east Asia, J. Geophys. Res., 112, D24S91, doi:10.1029/2007JD009009, 2007.

Phillips, B. L.: A technique for numerical solution of certain integral equation of first kind, J. Assoc. Comput. Mach., 9, 84–97, 1962.

Pope lii, C.A., Burnett, R.T., Thun, M. J., Calle, E. E., Krewski, D., Ito, K., and Thurston, G. D.: Lung cancer, cardiopulmonary mortality, and long-term exposure to fine particulate air pollution, J. Am. Med. Assoc, 287(9), 1132–1141, doi: 10.1001/jama.287.9.1132, 2002.

Ramanathan, V., Crutzen, P. J., Kiehl, J. T., Rosenfeld, D.: Aerosols, climate, and the hydrological cycle, Science, 294, 2119–2124, 2001.

Rodgers, C. D.: Inverse Method for Atmospheric Sounding, World Sci., Singapore, 240, 2000.

Samet, J.M., Zeger, S.L., Dominici, F., Coursac, I., Dockery, D.W., Schwartz, J., and Zanobetti, A.: The national morbidity, mortality, and air pollution study. Part II: morbidity and mortality from air pollution in the United States, Health Effects Institute, Cambridge MA, Research Report 94, 2000.

Sun, K., Liu, H. N., Wang, X. Y., Peng, Z., and Xiong, Z.: The aerosol radiative effect on a severe haze episode in the Yangtze River Delta., J. Meteor. Res., 31(5), 865–873, doi: 10.1007/s13351-017-7007-4, 2017.

Takamura, T., and Nakajima, T.: Overview of SKYNET and its activities, Opt. Pura Y Apl., 37, 3303–3308, 2004.

Twomey, S.: On the numerical solution of Fredholm integral equations of the first kind by the inversion of the linear system produced by quadrature, J. Assoc. Comput. Mach., 10, 97–101, 1963.

Turchin, V. F. and Nozik, V. Z. : Statistical regularization of the solution of incorrectly posed problems, Izv. Atmos. Ocean. Phy.+, **5**, 14–18, 1969.

Uchiyama, A., Yamazaki, A., Togawa, H., and Asano, J.: Characteristics of Aeolian dust observed by sky-radiometer in the Intensive Observation Period 1 (IOP1), J. Meteor. Soc. Japan, 83A, 291–305, doi: 10.2151/jmsj.83A.291, 2005.

Wang, Z. W., Yang, S. Q., Zeng, Q. L., and Wang, Y. Q.: Retrieval of aerosol optical depth for Chongqing using the HJ-1 satellite data, J. Meteor. Res., 31(3), 586 – 596, doi: 10.1007/s13351-017-6102-x, 2017.

Wang, Z. Z., Liu, D., Wang, Z., Wang, Y. J., and Khatri, P.: Seasonal characteristics of aerosol optical properties at the SKYNET Hefei site (31.90°N, 117.17°E) from 2007 to 2013, J. Geophys. Res., 119,

6128–6139, doi:10.1002/2014JD021500, 2014.

Zhao, B., Liou, K.-N., Gu, Y., Jiang, J. H., Li, Q., Fu, R., Huang, L., Liu, X., Shi, X., Su, H., and He, C.: Impact of aerosols on ice crystal size, Atmos. Chem. Phys., 18, 1065-1078, DOI 10.5194/acp-18-1065-2018, 2018a.

Zhao B., Jiang, J. H., Diner, D. J., Su, H., Gu, Y., Liou, K.-N., Jiang, Z., Huang, L., Takano, Y., Fan, X.H., and Omar, A. H.: Intra-annual variations of regional aerosol optical depth, vertical distribution, and particle types from multiple satellite and ground-based observational datasets, Atmos. Chem. Phys., 18, 11247–11260, doi:10.5194/acp-18-11247-2018, 2018b

Yang, Y. R., Liu, X. G., Qu, Y., An, J. L., Jiang, R., Zhang, Y. H., Sun, Y. L., Wu, Z. J., Zhang, F., Xu, W. Q., and Ma, Q. X.: Characteristics and formation mechanism of continuous hazes in China: A case study during the autumn of 2014 in the North China Plain, Atmos.Chem. Phys., 15, 8165–8178, doi: 10.5194/acp-15-8165-2015, 2015.

Atmos. Meas. Tech. Discuss., https://doi.org/10.5194/amt-2019-39
Manuscript under review for journal Atmos. Meas. Tech.
Discussion started: 6 March 2019

Atmospheric Measurement Techniques Discussions

Table 1. Averaged single scattering albedo and refractive index in SKYRAD 5.0 and 4.2, and the absolute and percentage differences between the two versions at Qionghai site during February 2013 to February 2015.

	400 nm	500 nm	670 nm	870 nm	1020 nm
$\omega_{v5.0}$	0.8676	0.8800	0.8824	0.8726	0.8662
$\omega_{v4.2}$	0.8970	0.8984	0.8856	0.891	0.8820
$m_{r\_v5.0}$	1.4726	1.4604	1.455	1.4785	1.475
$m_{r\_v4.2}$	1.4127	1.4269	1.4368	1.4578	1.4593
$m_{i\_v5.0}$	0.0188	0.0148	0.0120	0.0126	0.0126
$m_{i\_v4.2}$	0.0115	0.0102	0.0097	0.0078	0.0081
$\delta\omega$	−0.0294	−0.0184	−0.0032	−0.0184	−0.0158
δm_r	0.0599	0.0335	0.0182	0.0207	0.0157
δm_i	0.0073	0.0046	0.0023	0.0048	0.0045
$\delta\omega$%	−3.28%	−2.05%	−0.36%	−2.07%	−1.79%
$\delta m_{r\%}$	4.24%	2.35%	1.27%	1.42%	1.08%
R_{mi}	1.63	1.45	1.24	1.62	1.56

ω, m_r and m_i mean averaged single scattering albedo, real part of refractive index and the imaginary part of refractive index; subscript v5.0 and v4.2 mean parameters retrieved by SKYRAD V5.0 and V4.2, respectively; δ- and δ-% mean absolute and percentage difference between SKYRAD V5.0 and V4.2, respectively; R_{mi} means the ratio of $m_{i\_v5.0}$ to $m_{i\_v4.2}$.

Atmos. Meas. Tech. Discuss., https://doi.org/10.5194/amt-2019-39
Manuscript under review for journal Atmos. Meas. Tech.
Discussion started: 6 March 2019

Atmospheric Measurement Techniques Discussions

Table 2. The same as Table 1 but for Yucheng during February 2013 to February 2015.

	400 nm	500 nm	670 nm	870 nm	1020 nm
$\omega_{v5.0}$	0.8628	0.9135	0.9015	0.8620	0.8290
$\omega_{v4.2}$	0.8847	0.8853	0.8819	0.8955	0.8876
$m_{r\_v5.0}$	1.471	1.4628	1.4843	1.5453	1.5593
$m_{r\_v4.2}$	1.4937	1.5046	1.5071	1.5396	1.5337
$m_{i\_v5.0}$	0.01513	0.0070	0.0075	0.0126	0.0164
$m_{i\_v4.2}$	0.01243	0.0115	0.0100	0.0079	0.0081
$\delta\omega$	−0.0219	0.0282	0.0196	−0.0335	−0.0586
δm_r	−0.0227	−0.0418	−0.0228	0.0057	0.0256
δm_i	0.0027	−0.0045	−0.0025	0.0047	0.0083
$\delta\omega$%	−2.48%	3.19%	2.22%	−3.74%	−6.60%
$\delta m_{r\%}$	−1.52%	−2.78%	−1.51%	3.70%	1.70%
R_{mi}	1.22	0.61	0.75	1.59	2.02

ω, m_r and m_i mean averaged single scattering albedo, real part of refractive index and the imaginary part of refractive index; subscript v5.0 and v4.2 mean parameters retrieved by SKYRAD V5.0 and V4.2, respectively; δ- and δ-% mean absolute and percentage difference between SKYRAD V5.0 and V4.2, respectively; R_{mi} means the ratio of $m_{i\_v5.0}$ to $m_{i\_v4.2}$.